Control of carbon content in WC-Co hardmetal by heat treatment in reducing atmospheres containing methane.

S. R. Parker, M. J. Whiting, and J. A. Yeomans

Centre for Engineering Materials, Department of Mechanical Engineering Sciences, University of Surrey, Guildford, Surrey GU2 7XH, UK

February 7, 2017

Abstract

Pressed WC-Co hardmetal compacts of two different compositions, 6 and 10 wt.% Co, were heat treated under flowing atmospheres of nitrogen, hydrogen and methane at temperatures from 500 to 900 °C prior to sintering under argon. Microstructural examination showed excessive carburisation up to 2.5 mm into the compacts with regions most exposed to heat treatment atmospheres showing greatest carburisation. η-phase was present in the 6 wt.% Co samples heat treated at low temperatures without methane but was not present with heat treatment temperatures of 700 °C or above with methane present. The hardness of both materials was significantly lower in highly carburised regions, highlighting the need for careful control of heat treatment parameters.

1 Introduction

Unwanted variation in carbon concentration reduces the predictability of hardness and toughness in sintered hardmetal and has been of great concern to manufacturers of hardmetal components since at least the 1950s [2] [8]. Carbon content below the two phase region leads to the formation of brittle η-phase. The sensitivity of phase equilibria in the WC-Co system to carbon content is highest for low Co compositions. Phase diagrams showing the narrowing of the two-phase, δ-WC + α-Co, region are given in [12] and [5]. According to the phase diagram in [12], for a 6 wt.% Co WC-Co hardmetal the two-phase region is approximately ±0.01 wt.% at 1000 °C , a temperature below which further movement towards equilibrium will be slow after cooling after sintering at temperatures normally in excess of 1430 °C. It has been shown that heat-treating pressed compacts in carbonaceous atmospheres

can increase the carbon content of sintered hardmetal and thereby provide a route for some degree of carbon control [1] [8] [7] [6]. Increasing carbon content can reduce the hardness of the binder by reducing the quantity of dissolved tungsten but carbon content also affects grain size and morphology. Above a critical carbon content carbon precipitates will form which will create defects around which cracks may form and more easily propagate leading to loss of toughness.

Carburisation is a diffusion process and the rate at which it occurs is dependent on temperature as well as the concentration of carbon present [8]. Work showing that it is possible to influence the mechanical properties of sintered hardmetal by sintering in a hydrogen atmosphere with additions of methane has been reported [1]. The concentration of methane required to achieve carburisation without leading to abundant precipitation of carbon in sintered compacts is very sensitive to the heat-treatment temperature. Using a separate heat treatment step provides some advantages as hardmetal is more commonly sintered under a vacuum or argon, and many furnaces used for sintering cannot be easily modified to accept controlled flows of methane. Studies by Konyashin [7] [6] have shown that heat treatments under methane can produce hardmetal components with non-uniform microstructures. The carburising effect is stronger in the near surface region; in the manufacture of functionally graded materials this may be desirable.

Although the reported work has shown adding methane to heat-treatment atmospheres is a promising method, there is a need for improved understanding of the parameters that produce carbon contents within the range free of η-phase and carbon precipitates. The motivation for this study is the need for an improved scientific understanding of the potential for carbon control in WC-Co hardmetal by adding methane to flowing heat treatment atmospheres. This experimental investigation builds upon findings reported in [1] and [3] by adding methane to a flowing base gas of nitrogen and hydrogen, as is commonly used in the heat treatment of pressed compacts before green machining in commercial processing of hardmetals. When heat treatments lead to excessive carburisation samples will exhibit graphite in the microstructure and η-phase will be present when carbon content is not sufficiently increased to compensate for later carbon loss in compositions prone to η-phase. The experimental investigation aims to identify useful ranges for both heat-treatment temperature and methane flow rate that produce samples of high hardness but are free of η-phase which reduces toughness. It is not the aim of the work reported in this paper to produce functionally graded materials but the degree of carburisation will likely vary within samples. Measurements of mechanical properties will be made at different positions in samples to better understand this spatial variation.

2 Materials and methods

2.1 Sample preparation

Two different compositions of hardmetal were used in this investigation, the compositions of which are given in table 1. Particle sizes are mean particle diameters quoted by suppliers listed in table 1 obtained by Fischer sub size sieving (FSSS) or laser particle size analysis. The carbide powder listed in table 1 have small amounts of free carbon present. Manufacturers will sometimes over carburise powders as carbon gets lost in the manufacture of hardmetal. For the cobalt the carbon, the carbon is a small amount of contamination. Overall purity of the cobalt powder 99.7 wt.% .

Composition A was chosen for simplicity, containing only tungsten carbide and cobalt in proportions very typical of hardmetal. Composition B is lower in cobalt and, therefore, more susceptible to η-phase formation due to narrowing of the δ-WC + α-Co two-phase window making better carbon control more important and changes in carbon content more apparent [11]. Lower cobalt content and the presence of the grain growth inhibitors, NbC and TaC, are typical of highly wear resistant commercial hardmetal compositions.

Table 1: The powder compositions used to make samples for treatments.

A						
Amount (wt.%)	Material	Mean particle diameter (μm)	Total C (wt.%)	Total C (at.%)	Free C (wt.%)	Supplier
90.0	WC	3.5	6.12 (6.12-6.16)	49.79 (49.97-50.14)	0.02	HC Starck
10.0	Co	1.2	0.013	-	0.013	Nanjing Hanrui Cobalt

B						
Amount (wt.%)	Material	Mean particle diameter (μm)	Total C (wt.%)	Total C (at.%)	Free C (wt.%)	Supplier
73.5	WC	1.7	6.14 ±0.02	50.05 ±0.3	0.04	HC Starck
20.0	WC	3.2	6.14 ±0.02	50.05 ±0.3	0.02	HC Starck
6.0	Co	1.2	0.013	-	0.013	Nanjing Hanrui Cobalt
0.3	Ta/NbC (90/10)	1.8	6.72	50.82	0.12	Sandvik
0.2	NbC	2.5	11.29	49.63	0.12	Sandvilk

Each sample was pressed from powders milled in an industrial scale hardmetal manufacturing facility. Batches of 100 kg of powder were milled together for 48 hours in a steel-lined attritor mill using acetone and fine grained tungsten carbide milling balls approximately 5 mm in diameter as a milling medium. Once removed from the mill, the acetone was removed from the slurry by heating in an oven at 300 mbar and 60 °C for 6 hours. Paraffin wax mixed into the dried powder blend at a 1:50 mass ratio using approximately 3 litres of trichloroethylene as a solvent. The mixture was dried again as previously but at 850 mbar to evaporate the trichloroethylene. Agglomerates were broken down by vibratory sieving using an 800 μm then a 600 μm sieve. Powders were then granulated by air-drying in a rotating drum. Cylindrical pellets 10 mm in diameter and approximately 5 mm in height were pressed in a uniaxial, single-action press at 500 MPa.

2.2 Heat treatments of samples

To investigate the effects of heat-treatment temperature a fixed methane flow rate of 0.1 l min^{-1} was used with the range of heating cycles shown in figure 1. To investigate the effects of methane flow rate the heat treatment temperature was set to 800 °C and the methane flow rate varied between 0 and 0.1 l min^{-1}

The furnace used for heat treatments was a Carbolite GHA12/450 tube furnace with an alumina work tube with a 50 mm internal diameter. Gas flows were controlled using gravimetric flow meters. The base gas entering the tube furnace was a 50:50 mixture of nitrogen:hydrogen and had a flow rate of 2 l min^{-1}. Hydrogen prevents oxidation of pressed compacts and the nitrogen is present because cracked ammonia is often used as the hydrogen source in commercial operations which this experiment aims to simulate though in this investigation gasses came from separate bottles with independent flow controls. The protective atmosphere also prevents

combustion of the wax plasticiser, which would leave carbon deposits. Methane was added to this flowing atmosphere without any reduction in the flow rate of the base gas so the total flow rate increased by up to 5% . Accuracy of flow control for the hydrogen and nitrogen was ± 0.01 l min^{-1} and for the methane ± 0.001 l min^{-1} as rated by the manufacturer of the gas flow controllers. Samples were placed in alumina boats with the bottom face marked to allow properties in different regions within samples to be related to orientation during heat treatment.

All heat treatments began with a two-hour hold at 410 °C to remove the wax plasticiser. A constant ramp rate of 4 °C min^{-1} was used during the heating cycle. Consequently, heat treatments at higher temperature were longer so for this investigation heat treatment temperature and duration are not independent. Peak heat treatment temperatures were maintained for two hours followed by unforced cooling to room temperature. Gas flows were maintained until the thermocouple built-in to the furnace gave a reading below 50 °C. Each sample was weighed before and after heat treatment to determine if increase in carbon content was large enough to be observed in mass measurements.

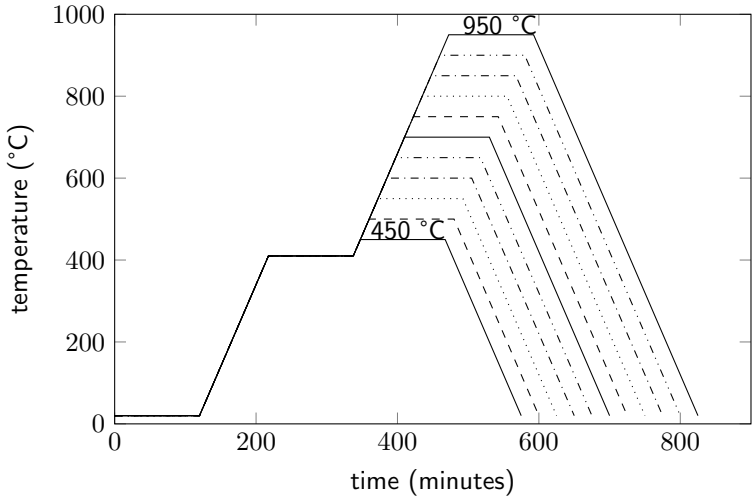

Figure 1: Heating programmes used for the heat treatments each done with and without methane. Actual cooling rates will reduce as temperature decreases. The heat treatment where SP=800 °C was used to study the effects of varying methane content.

2.3 Sintering of samples

Samples were sintered in a small vertical loading furnace in a stack of alumina dishes. The furnace chamber was flushed with argon for 30 minutes prior to commencing the heating cycle and was kept under an argon atmosphere at a pressure of 1 atm.

throughout the sintering cycle. The use of this atmosphere was based on availability of laboratory scale equipment. A ramp rate of 50 °C min^{-1} was used up to 1150 °C. This temperature was held for 35 minutes as is often done in commercial production to allow for some degree of solid-state sintering to take place before starting liquid-phase sintering. A ramp rate of 20 °C min^{-1} was used up to the sintering temperature of 1450 °C. After completion of the sintering cycle the furnace was allowed to cool freely; no cooling gas was injected.

2.4 Density

Density measurements can provide information on the level of porosity as well as carbon content. Porosity and excess carburisation decrease density but high density can also indicate carbon deficiency. Sintered samples were ultrasonically cleaned in purified water to remove surface contaminants and density measurements made using the Archimedes method. Dry and immersed mass measurements were each made three times and a mean used. By examining variation in the mass measurements of the same sample an estimated error of $\pm$ 0.06 g cm^{-3} was calculated. Density measurements are an average over each sample do not provide information on variation within samples.

2.5 Microstructural analysis

Sintered samples were sectioned, mounted in Bakelite and polished using standard metallographic preparation procedures for hardmetal. The final polishing stage used 0.04 µm silica colloid polishing media. Samples were examined using a Jeol 7100F SEM with an accelerating voltage of 5 kV. The use of a low accelerating voltage leads to contrast between tungsten carbide grains of different orientation and allowed grain size to be determined by the mean linear intercept method. A Zeiss LSM 700 confocal laser scanning microscope (CLSM) was used to determine the depth to which carbon was deposited in samples and to generally assess the effects of the various heat treatments on the final microstructure.

2.6 Microhardness

Micro-Vickers hardness indentations were made using a load of 2 kgf at intervals of approximately 0.5 mm along straight lines between the edges of sample sections corresponding to the top and bottom sample face. The sizes of sample indentations were measured on images captured on the CLSM. Microscope automation enabled combining images of high enough magnification to measure individual indentations into larger images which could be used to measure the position of indentations relative to the top sample surface, in addition to hardness. Figure 2.2 shows a line of indentations made in a sample of composition B heat treated at 800 °C with 0.05 l min^{-1} CH_4. Two composite images of each line were captured to ensure a high quality image of each indent was available. Creating composite images allowed a resolution of 0.25 µm per pixel to be acquired over a length of around 5 mm.

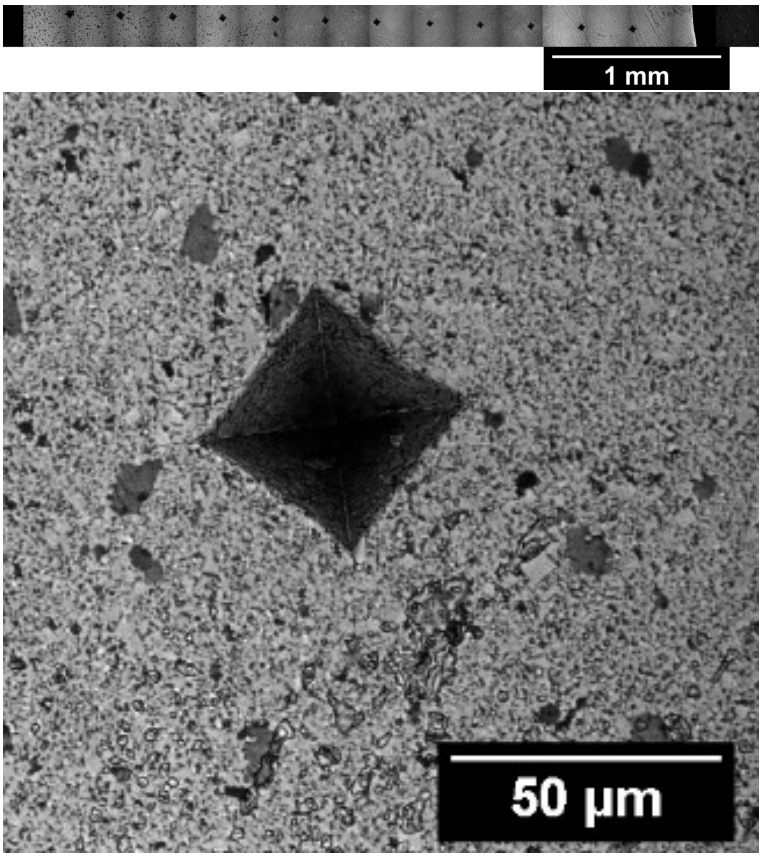

Figure 2: (Top) A line of Vickers microhardness indentations in a sample of composition B heat treated at 800 °C with 0.05 l min^{-1} CH_4 . The left side of the sample was most exposed to the atmosphere during heat treatment whereas the left side was face down in the alumina boat. The composite images are used to determine the positions of indentations. (Bottom) Third indentation from the left in the line on indentations.

2.7 Magnetic moment

Determination of binder phase composition was limited to magnetic moment measurements, a method commonly used in the hardmetal industry [9]. The magnetic moment of pure cobalt is 16.1 µ T m^3 kg^{-1} but this is reduced as the amount of tungsten dissolved in the binder phase increases [11]. Roebuck [10] proposed an equation relating the magnetic moment of the binder phase to the amount of tungsten dissolved in the cobalt. See equation 1, below, where σ_B is the magnetic moment of the binder phase in µT m^3 kg^{-1}, σ_{Co} is the magnetic moment of pure cobalt and m_W is the amount of dissolved tungsten in wt.%. [10]. The coefficient of 0.275 was derived empirically by Roebuck [10]. In the same work coefficients for

other dissolved metals, but not for niobium or tantalum, are reported from other literature. For the purposes of the work reported here it is assumed no tantalum or niobium is dissolved in the binder phase.

$$\sigma_B = \sigma_{Co} - 0.275 m_W \tag{1}$$

The amount of carbon dissolved in the binder phase can be inferred from the amount of dissolved tungsten; dissolved tungsten decreases with increasing dissolved carbon [11]. Direct measurement of the carbon content of the binder phase is difficult due the presence of carbide grains and the often sub-micron mean free path. Soares reports the two phase region, free of carbon precipitates and η-phase, has a binder magnetic moment of 11.5 - 15.6 μT m^3 kg^{-1} [11]. Using equation 1 this gives a dissolved tungsten content of 1.8 - 16.7 wt.%.

Magnetic moment measurements were made on samples before any sectioning or metallographic preparation. The mass of each sample was measured to an accuracy of $\pm$0.001 g and the binder fraction was taken to equal the proportion of cobalt powder in the hardmetal powder blend, 10 wt.% for composition A and 6 wt.% for composition B. Magnetic moment measurements were performed on a Magnetech Magnetic Moment Integrator and it was assumed the strength of the magnetic field was sufficient to completely magnetise samples.

3 Results

3.1 Effects of heat treatment temperature

3.1.1 Density

As shown in figure 3 The sintered densities of samples of compositions A and B fall slightly when 0.025 l min^{-1} compared to heat treatment without methane. Without methane the sample of composition A has a sintered density of 14.58 g cm^{-3} with the addition of 0.025 l min^{-1} CH_4 sintered density falls to 14.46. With increasing CH_4 flow rate density decreases rapidly to 13.05 g cm^{-3} in composition A. In samples of composition B the sintered density of samples heat treated without CH_4 is 14.92 g cm^{-3} and falls to 13.35 g cm^{-3} with 0.1 l min^{-1} CH_4.

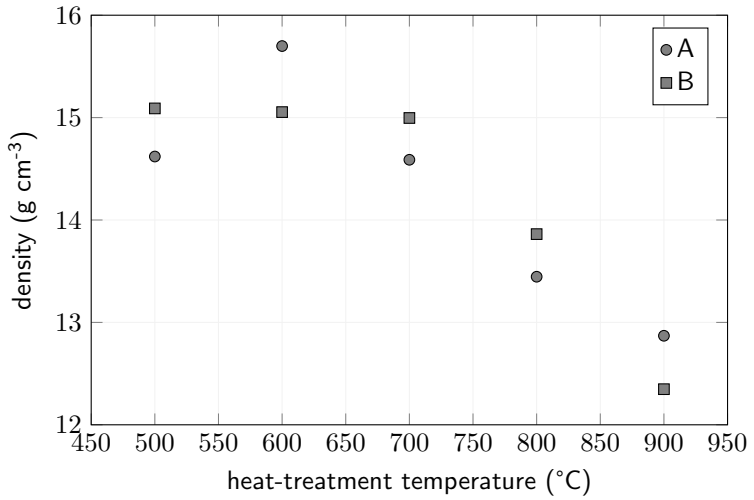

Figure 3: Densities of samples heat treated under 0.1 l min^{-1} CH_4 at temperatures ranging from 500 to 800 °C. Estimated errors are ± 0.06 g cm^{-3}.

3.1.2 Microstructural analysis

Examination of samples by CLSM showed the depth of carburisation increased with heat treatment temperature, noting higher temperature meant longer heat treatments for this investigation. Heat-treatment temperatures investigated ranged from 500 – 900 °C. η-phase was present in samples of composition B heat treated at 500 and 600 °C. No η-phase was present in samples of composition A. With 0.1 l min^{-1} CH_4 carburisation was excessive with heat treatment temperature above 700 °C. Samples showed graphite precipitation at depths of up to 2.5 mm from the surface most exposed to the heat treatment atmosphere. Carburised samples also showed increased mass after accounting for the evaporation of the wax plasticiser. A compact of composition A heat treated at 700 °C with 0.1 l min^{-1} showed a mass decrease of 2.0 %, corresponding to the evaporation of wax plasticiser and some additional mass loss, and had a carbon content after heat treatment of 6.0 wt.% as measured by the infra-red gas absorption method described in [4]. A sample of the same composition heat treated at 850 °C decreased in mass by 0.3 % and had a carbon content after heat treatment of 7.4 wt.%. These results suggest mass increase after wax removal is attributable to carburisation.

3.1.3 Microhardness

The sample of composition A, heat treated at 500 °C under 0.1 l min^{-1} CH_4, exhibited hardness values ranging from 1340 to 1430 H_{V2}. For composition B from the same heat treatment the hardness varied from 1644 to 1725 H_{V2}. In samples heat treated with 0.1 l min^{-1} CH_4 hardness did not change significantly with heat-treatment temperature below 800 °C but, as clearly shown in figure 4, for 800 °C

and above hardness was greatly reduced in the region closest to the face most exposed to the heat treatment atmosphere and to a lesser extent the opposite face, that touching the alumina boat during heat treatment and sintering.

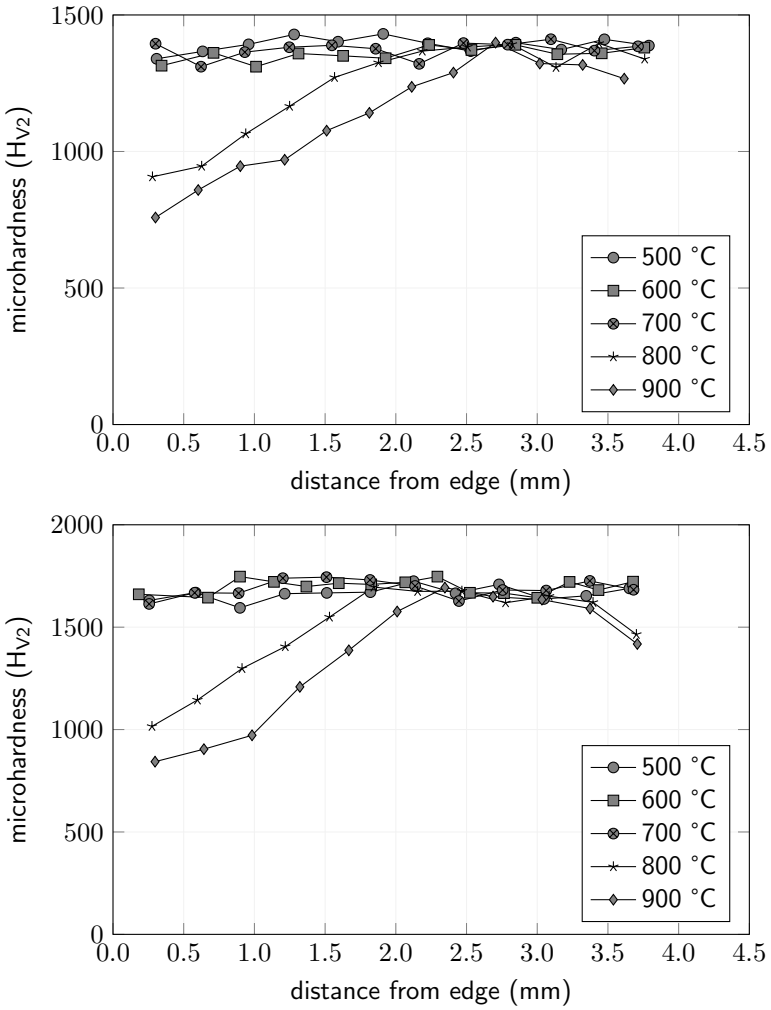

Figure 4: Microhardness at different distances from the upper sample face in samples heat treated under 1 l min^{-1} H_2, 1 l min^{-1} N_2, 0.1 l min^{-1} CH_4 using temperatures ranging from 500 - 900 °C. (Top) Composition A, (bottom) composition B. For heat treatment temperatures of 700 °C and above the magnitude and depth of hardness decreases increases with temperature.

3.1.4 Magnetic moment

Figure 5 shows the specific magnetic moment of the binder phase increases, indicating decreasing dissolved tungsten, with heat treatment temperatures between 600 and 800 °C. Above and below these temperatures magnetic saturation appears to remain essentially unchanged. This indicates that the binder composition in sintered samples is strongly affected by the heat treatment temperature used. If control of carbon was to be achieved within the compositional range, free of η-phase and carbon precipitates the optimum temperature for heat treatment would apparently lie between 600 and 800 °C for this particular experimental setup. The error of ± 0.02 μT m^3 kg^{-1} is an estimate. Readings are generally consistent within 1% and there will be a small error on the measurement of the mass of each sample.

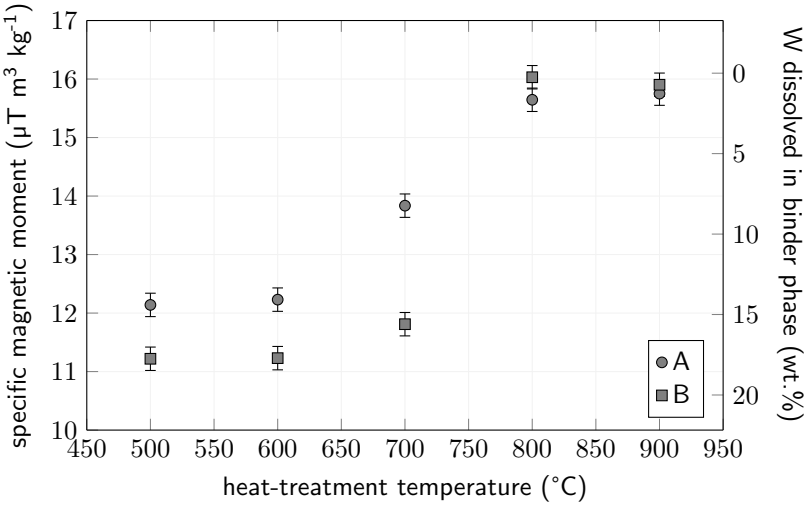

Figure 5: Specific magnetic moment of the binder phase of samples heat treated under 0.1 l min^{-1} CH_4 at temperatures ranging from 500 to 800 °C. The corresponding amount of dissolved tungsten is calculated from equation 1

3.1.5 Discussion

Upper and lower limits for heat-treatment temperatures within which the range for producing samples free of carbon precipitates and η-phase with a CH_4 flow rate of 0.1 l min^{-1} have been determined. Microstructural analysis has shown that in samples of composition B a heat treatment at 600 °C or below leads to samples with η-phase present and at 800 °C and above graphite is present. This indicates the optimal temperature for producing samples free of graphite is around 700 °C. η-phase is not present in any samples of composition A so a lower limit cannot be determined from microstructural analysis.

Samples heat treated at 800 °C and above exhibited significantly reduced hard-

ness to a depth of around 2 mm in both compositions. This reduction in hardness would not be acceptable for commercial manufacturers of hardmetal components as plastic deformation and wear would dramatically increase. Hardness is much more uniform at 700 °C further supporting the conclusion drawn from microstructural analysis that this lies close to the optimal processing temperature for composition B.

The magnetic saturation of the binder phase of both compositions also indicate that samples free of graphite and η-phase can be produced with heat treatments between 600 and 800 °C as these temperatures mark the upper and lower limits of the magnetic moment. In composition A magnetic moment of the binder phase varied between 12.2 - 15.8 μT m^3 kg^{-1} and in composition B it varied between 11.2 - 15.9 μT m^3 kg^{-1} which both roughly equate to the limits proposed in [11] for the two-phase region, 11.5 - 15.6 μT m^3 kg^{-1}.

More heat treatments should be done to further narrow the range of heat-treatment temperatures that produce samples free of graphite and η-phase now a broad range has been determined. It may also be possible to determine a relationship between heat-treatment temperature and the amount of dissolved tungsten in the binder phase. High levels of dissolved tungsten, corresponding to low carbon, increases hardness whilst low levels of dissolved tungsten increase toughness. Both could be beneficial in different applications. Further work would also be needed to determine if uniform samples could be produced.

3.2 Effects of methane flow rate

3.2.1 Density

As shown in figure 6 The sintered densities of samples of compositions A and B fall slightly when 0.025 l min^{-1} compared to heat treatment without methane. Without methane the sample of composition A has a sintered density of 14.58 g cm^{-3} with the addition of 0.025 l min^{-1} CH_4 sintered density falls to 14.46. With increasing CH_4 flow rate density decreases rapidly to 13.05 g cm^{-3} in composition A. In samples of composition B the sintered density of samples heat treated without CH_4 is 14.92 g cm^{-3} and falls to 13.35 g cm^{-3} with 0.1 l min^{-1} CH_4.

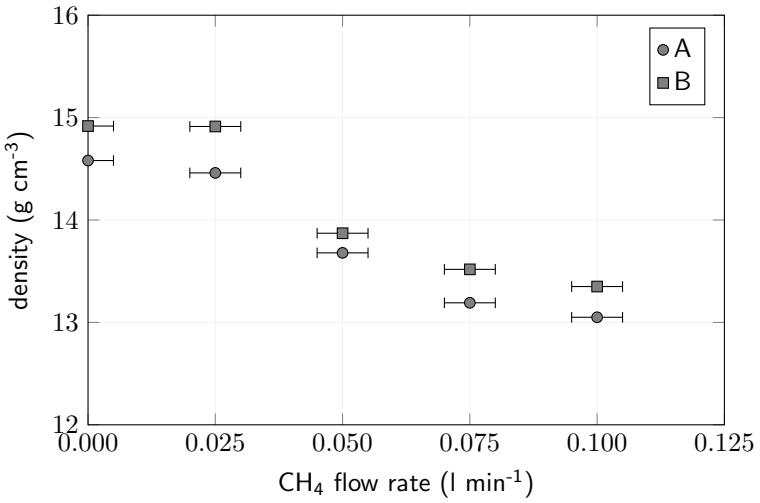

Figure 6: Densities of samples heat treated at 800 °C with flow rates of CH_4 up to 0.1 l min^{-1} in an atmosphere of 1 l min^{-1} N_2 and 1 l min^{-1} H_2. Estimated errors are $\pm$0.06 g cm^{-3}.

3.2.2 Microstructural analysis

Again, there was no η-phase apparent in any samples of composition A. Qualitative microstructural examination using CLSM showed the sample of composition B heat treated without methane and the sample heat treated with 0.025 l min^{-1} CH_4 showed η-phase in the microstructure. With higher CH_4 flow rates no η-phase was visible. With 0.05 l min^{-1} CH_4 the depth of carburisation was around 3 mm in composition A and 2 mm in composition B. With 0.1 l min^{-1} CH_4 samples showed graphite precipitates throughout.

Figure 7 is a low keV secondary electron image of three sintered samples of composition B heat treated at 800 °C with 0.025, 0.05 and 0.075 l min^{-1} CH_4. The mean linear intercept of tungsten carbide grains calculated from the images shown in figure 7 are 1.17 µm for 0.025 l min^{-1} CH_4, 1.21 µm for 0.05 l min^{-1} CH_4 and 1.12 µm for 0.075 l min^{-1} CH_4. Grain size does not appear to increase with increasing methane flow rate. This could be because the carbon content is already high enough to cause graphite precipitation with a CH_4 flow rate of 0.025 l min^{-1} and higher flow rates have no other effect of microstructure other than to increase graphite precipitation. No distinct bi-modal distribution was seen even though composition B has 73.5 wt.% 1.1 µm and 20 wt.% 3.2 µm WC. This is likely due to the small number of large grains in the images. Images suitable for grain size measurement were only collected at the centre of samples so comparison of grain size in different regions was not possible.

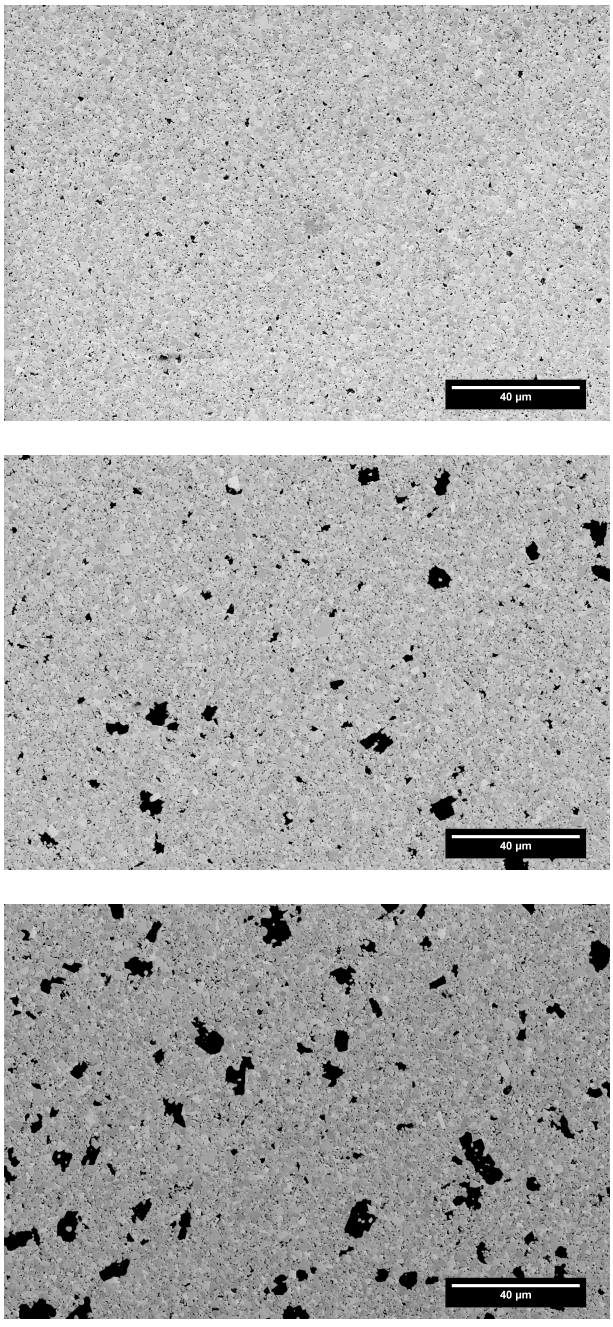

Figure 7: Secondary electron micrographs taken at 5 keV of sintered and polished samples of composition B heat treated at 800 °C with different methane flow rates; (top) 0.025 l min^{-1}, (middle) 0.050 l min^{-1}, (bottom) 0.075 l min^{-1}. Graphite indicated by black regions are larger and more prevalent in samples heat treated with higher methane flow rates. Micrographs are from the centres of samples and the degree of carbon precipitation varies within samples.

3.2.3 Microhardness

Overall hardness was found to decrease with increasing methane flow rate. Hardness was lower in the region nearest the face most exposed to the heat treatment atmosphere and this was most marked in samples heat treated with 0.05 l min^{-1} CH_4 where hardness in the inner regions matched that of the sample heat treated without methane whilst at the top face is was 400 H_V lower for composition A and around 600 H_V lower in composition B. There were two supposedly identical heat treatments with a heat-treatment temperature of 800 °C and a CH_4 flow rate of 0.1 l min^{-1} CH_4, one for investigating the effect of heat-treatment temperature and the other for investigating the. Hardness does not rise as steeply with distance from the top surface in samples heat treated in the investigation into the effect of CH_4 flow rate. This difference could indicate an issue in controlling gas flow rates or other parameters of heat treatments.

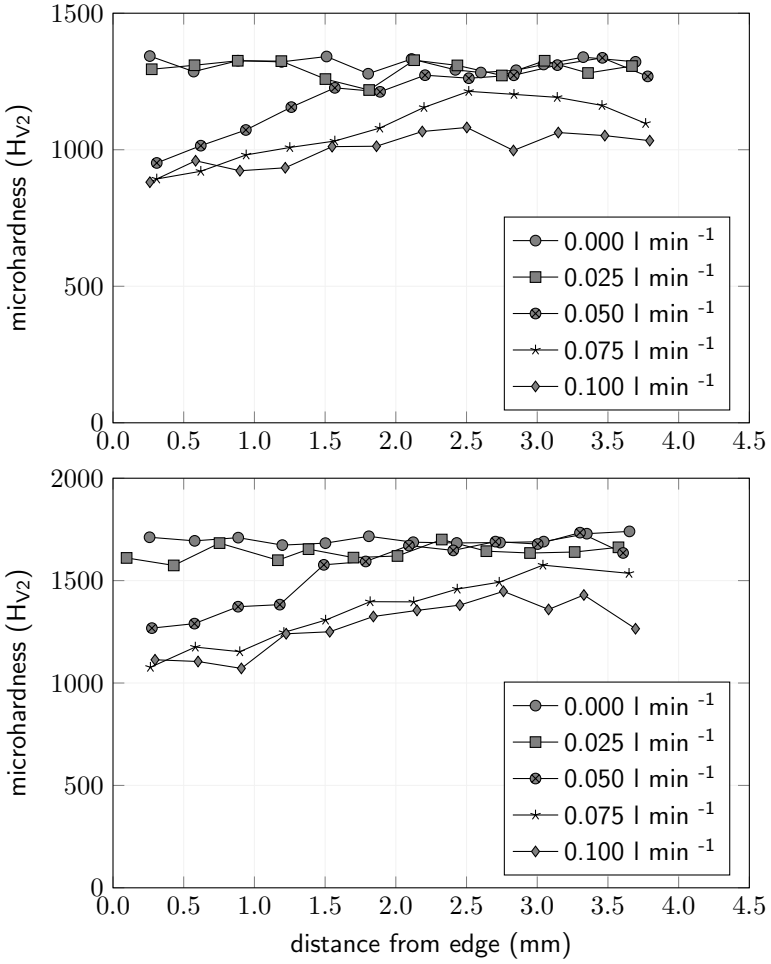

Figure 8: Microhardness at different distances from the upper sample face in samples heat treated under 1 l min^{-1} H_2, 1 l min^{-1} N_2 at 800 °C with CH_4 added at flow rates ranging from 0 - 0.1 l min^{-1}. (Top) Composition A, (bottom) composition B. At the highest flow rates hardness is reduced CH_4 throughout. At intermediate flow rates hardness is reduced to a greater extent close to the top sample face.

3.2.4 Magnetic moment

Magnetic moment measurements from the investigation into the effects of methane flow rate are given in figure 9. The magnetic moment of the binder phase reaches a maximum of around 15.4 μT m^3 kg^{-1} in composition A at 0.025 l min^{-1} CH_4 compared to 11.0 μT m^3 kg^{-1} for the sample heat treated without any CH_4. In composition B the maximum is reached at 0.05 l min^{-1} and there is a clear intermediate value of 14.4 μT m^3 kg^{-1}. Results suggest control of carbon content within

the compositional region free of η-phase and carbon precipitates can be achieved in composition A with a flow rate of 0.025 l min^{-1} or less and 0.050 l min^{-1} or less for composition B.

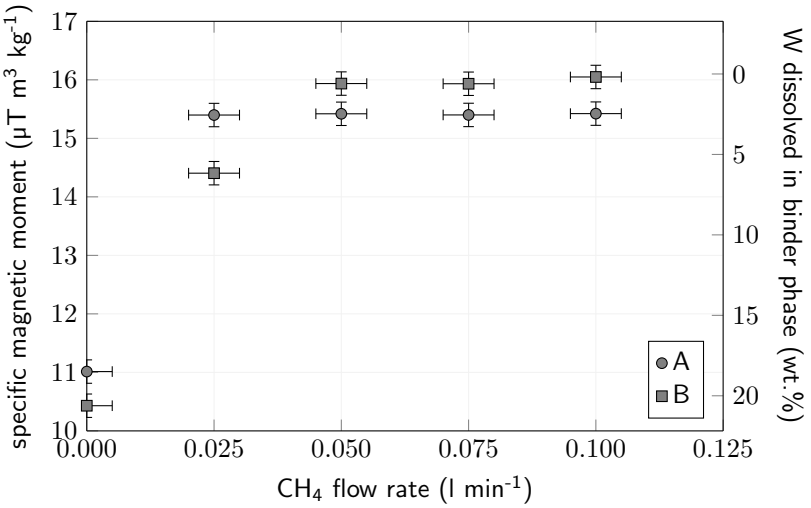

Figure 9: Specific magnetic moment of the binder phase of samples heat treated at 800 °C with flow rates of CH_4 up to 0.1 l min^{-1} in an atmosphere of 1 l min^{-1} N_2 and 1 l min^{-1} H_2. The corresponding amount of dissolved tungsten is calculated from equation 1.

The presence of η-phase in samples of composition B heat treated with 0.025 l min^{-1} CH_4 indicates a lower limit of CH_4 flow rate in producing samples free of η-phase. The presence of graphite in samples of both compositions with CH_4 flow rates of 0.05 l min^{-1} and above indicates an upper limit for producing samples free of graphite. There is no lower limit for composition B as there is no η-phase present and it may not be beneficial to heat-treat with methane at all. The large reduction in hardness of samples heat treated with 0.05 l min^{-1} CH_4 relative to samples heat treated without any CH_4 also indicates that this flow rate is detrimental.

The magnetic moment of the binder phase varies between 11.0 and 15.4 μT m^3 kg^{-1} for composition A and 11.0 to 16.0 μT m^3 kg^{-1} in composition B. Again, closely approximating the limits of the two-phase region reported in [11]. In composition A, the magnetic moment is close to maximum with a CH_4 flow rate of 0.025 l min^{-1} suggesting this could be close to the upper limit for avoiding graphite precipitation. For composition B, this does not occur until 0.05 l min^{-1}. It is not understood why the two compositions behave differently.

Within the limits of methane flow rates found here, 0 - 0.025 l min^{-1} for composition A and 0.025 - 0.05 l min^{-1} for composition B, will lie a narrower region within

which the binder phase composition can be controlled without introducing graphite or η-phase. Further investigations may be undertaken to identify this narrower range and to investigate the behaviour of different hardmetal compositions. As is also the case in investigating the effects of heat-treatment temperature, future work should also include measurement of fracture toughness.

4 Conclusions

- Heat treatments of pressed hardmetal compacts in methane-containing reducing atmospheres can increase carbon content.
- The temperature of heat treatment and the flow rate of methane affect the magnitude and depth of carburisation.
- Excessive carburisation leads to very significant drop in hardness and would need to be prevented in commercial application of similar heat treatments.
- Even though the two different compositions examined were quite different the depth and degree of carburisation appeared to be very similar.
- Parameters that increase carbon content sufficiently to eliminate η-phase without causing carbon precipitation in sintered samples have not been firmly identified but a range of heat treatment temperatures, 600 - 800 °C define a likely lower and upper limit for a CH_4 flow rate of 1 l min^{-1} noting again that heat treatment time increases with temperature for this investigation because of the use of fixed ramp rates.

5 Acknowledgements

Staff at Dymet Alloys are thanked for their help in producing samples for this research. Ken Mingard at NPL is thanked for help in acquiring SEM images.

Funding:

This work was supported by the Engineering and Physical Sciences Research Council (EPSRC); and Dymet Alloys a division of Corewire Limited. [EPSRC Grant reference number: EP/G037388/1].

References

[1] VP Bondarenko and EG Pavlotskaya. Hydrogen-containing chemically active gas medium for controlling carbon content of tungsten-base hard alloys. *International journal of hydrogen energy*, 22(2):205–212, 1997.

[2] Joseph Gurland. A study of the effect of carbon content on the structure and properties of sintered WC-Co alloys. *Transactions AIME*, 200:285–290, 1954.

[3] ASM International. *ASM Handbook, Volume 07 - Powder Metal Technologies and Applications*, chapter Production Sintering Practices. ASM International, 1998.

[4] Steel and iron - determination of total carbon content - infrared absorption methods after combustion in an induction furnace. Standard, BSI, 2001.

[5] T Johansson and B Uhrenius. Phase equilibria, isothermal reactions, and a thermodynamic study in the Co-WC system at 1150°C. *Metal Science*, 12(2):83–94, 1978.

[6] I Konyashin, S Hlawatschek, B Ries, F Lachmann, A Sologubenko, and T Weirich. A new approach to fabrication of gradient WC-Co hardmetals. *International Journal of Refractory Metals and Hard Materials*, 28(2):228–237, 2010.

[7] I Konyashin, B Ries, F Lachmann, and A T Fry. Gradient WC-Co hardmetals: Theory and practice. *International Journal of Refractory Metals and Hard Materials*, 36:10–21, 2013.

[8] Igor Konyashin. *Comprehensive Hard Materials*, chapter Cemented Carbides for Mining, Construction and Wear Parts. Elsevier, 2014.

[9] B Roebuck. Magnetic moment (saturation) measurements on hardmetals. *International Journal of Refractory Metals and Hard Materials*, 14(5):419–424, 1996.

[10] B Roebuck, M Gee, EG Bennett, and R Morrell. Measurement good practice guide no. 20. Technical report, National Physical Laboratory, 1999.

[11] Eduardo Soares, Luis F Malheiros, Joaquim Sacramento, Manuel A Valente, and Filipe J Oliveira. Microstructures and properties of submicrometer carbides obtained by conventional sintering. *Journal of the American Ceramic Society*, 95(3):951–961, 2012.

[12] Gopal S Upadhyaya. *Cemented tungsten carbides: production, properties and testing*. William Andrew, 1998.